THE JOURNAL OF PHYSICAL CHEMISTRY C

Article

pubs.acs.org/JPCC

Formation and Characterization of Femtosecond-Laser-Induced Subcluster Segregated Nanoalloys

Zhen Jiao,[†,‡] Mugunthan Sivayoganathan,[‡] Walter W. Duley,[‡,§] Peng He,*[,†] and Y. Norman Zhou*[,‡,∥]

[†]State Key Laboratory of Advanced Welding Production Technology, Harbin Institute of Technology, Harbin 150001, China

[‡]Centre for Advanced Materials Joining, [§]Department of Physics & Astronomy, and [∥]Department of Mechanical and Mechatronics Engineering, University of Waterloo, Waterloo, Ontario N2L 3G1, Canada

ABSTRACT: We report the first synthesis of subcluster segregated nanoalloys formed through the joining of immiscible metallic nanoparticles (NPs) using femtosecond (fs) laser irradiation. Immiscible alloy components consisting of Ag and Ni, and Ag and Fe, all in the form of NPs, were first deposited on a carbon film in vacuum by fs laser ablation from the parent metals. These samples of randomly distributed NPs were then irradiated with multiple fs laser pulses at a fluence of 1.5 mJ/cm^2. Transmission electron microscopy (TEM) observations indicate that Ag and Ni as well as Ag and Fe NPs were successfully joined under these conditions. Energy dispersive X-ray (EDX) results show that no mixing layer exists at the interface. The nanostructure in the interface reveals the assumption of a specific angle between two matching planes on either side of the interface. Calculation of the lattice mismatch indicates that the system adjusts to this angle so as to reduce surface energy. Structural ledges were also formed at the interface to further compensate for the atomic misfit.

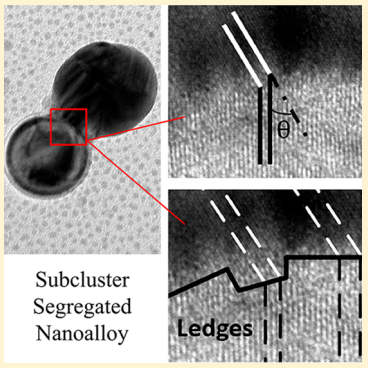

1. INTRODUCTION

Metallic NPs have widespread applications in materials science, chemistry, and biology due to their unique characteristics.[1−4] There is, correspondingly, much interest in nanoalloys, since the mixing of two or more metals over nanoscale dimensions offers many new opportunities for tailoring physical and chemical properties. Unique nanoalloys exhibiting novel characteristics can be obtained by accurately controlling NP size, composition, morphology, and atomic order. The possible structures can be classified as (1) core−shell, (2) mixed, (3) subcluster segregated, and (4) multishell nanoalloys.[5] Many experimental and theoretical studies have been carried out on these different types of nanoalloy.[6−10] All four types of structure are in principle possible, but there is little experimental evidence to date for subcluster segregated nanoalloys.[11,12] Subcluster segregated nanoalloys consist of two dissimilar nanoclusters, which share a mixed interface or a number of bonds.[5] Our recent work has outlined the synthesis of a subcluster segregated nanoalloy with a mixed Al−Fe interface.[13] However, there is yet no experimental evidence for bond sharing subcluster segregated nanoalloys.

Joining of dissimilar metallic NPs is one possible method to form subcluster segregated nanoalloys. Most previous work on this subject has focused on the simulation of joining in free dissimilar clusters.[11,12] However, few investigations have been carried out in terms of joining supported NPs, which is of great importance in the field of surface nanostructuring.[14] An important factor in joining at the nanoscale is precise control of melting depth in NPs,[15] preventing the NPs from merging to form a single particle.[16] Femtosecond (fs) laser irradiation is promising in this context since nonthermal effects dominate during short pulse irradiation.[15,17] We have verified this aspect of fs laser irradiation in our previous study of the joining of Al and Fe NPs.[13]

Immiscible materials are characterized by a large positive heat of mixing, resulting in little or no solubility of the two constituent elements.[18] As a result, core−shell segregated Ag−Ni nanoalloys have been formed in previous experiments.[19,20] To widen this study, the joining of immiscible Ag and Ni as well as Ag and Fe NPs has been investigated in our current experiments. As the formation and characterization of alloys between immiscible elements are attracting much scientific and technological interest, an investigation of joining between NPs involving immiscible components will contribute to a better understanding of alloying. Such particles may also have unique optical and catalytic properties that can be tailored to optimize engineering applications. For example, the ability to "tune" the plasmon resonance in structures assembled from these heterogeneous components is expected to open up new technology for light harvesting.[21] Thermal reconstruction in these materials introduces another controllable parameter with potential applications in the design of metamaterials.[22]

In this work, we present the first experimental evidence of bond sharing subcluster segregated nanoalloy created by exposure to fs laser irradiation. The nanostructure of Ag−Ni and Ag−Fe joints is characterized, and the mechanisms giving rise to this structure are discussed. These results provide a new approach to generate subcluster segregated nanoalloys, which

Received: July 3, 2014
Revised: October 7, 2014
Published: October 7, 2014

dx.doi.org/10.1021/jp506617f | J. Phys. Chem. C 2014, 118, 24746−24751

may enable a wide variety of applications since there are many possible combinations of metallic nanoparticles when immiscible materials are taken into account. In addition, this study provides useful new information on the mechanism of joining immiscible elements at nanoscale, which may facilitate connections in nanoalloy structures with specific properties.

2. EXPERIMENT

The experiments included preparation and joining of metallic NPs in vacuum with an fs laser system (1 kHz, 800 nm, Coherent, Inc.). The maximum pulse energy was 3.5 mJ at a pulse duration of 35 fs. NPs were first deposited on an ultrathin carbon film (400 mesh, <3 nm carbon film, copper TEM grid, Ted Pella) in a vacuum at room temperature by fs laser ablation. Ablation conditions were optimized to obtain a uniform, but dilute, distribution of each type of NP deposited on the substrate. We have found that an excessively dense distribution of NPs results in many overlapping NPs, which complicates the study of the fs-laser-induced joining process. Too dilute a deposition of NPs is also not ideal as few particles are close enough for joining. Studies show that experimental conditions during laser ablation, such as wavelength, pulse duration, irradiation time, and laser fluence, are factors that determine the NP size and production rate.[23,24] A series of experiments were carried out to determine the optimized ablation parameters for each material. The laser fluence and irradiation time for Ag (99.99%, Kurt J. Lesker), Ni (99.99%, Sigma), and Fe foil (99.99%, Sigma) are listed in Table 1.

Table 1. Optimum Ablation Parameters for Different Materials

material	Ag	Ni	Fe
laser fluence (mJ/cm^2)	216	127	89
irradiation time (s)	10	3	3

The resulting NPs were then exposed to fs laser irradiation to investigate the joining process. By testing a series of parameters, irradiation for 5 s (5000 overlapping pulses) to 10 s at a fluence between 1.5 and 2.2 mJ/cm^2 could get a considerable amount of joined NPs. At these fluence, the diameter of the laser spot was around 1 cm, which covered the entire substrate so that all the particles on the substrate were exposed to laser radiation. To study the joining of dissimilar metallic NPs, two continuing ablation were carried on with two different material targets but deposited onto the same substrate. This resulted in composite nanofilms with well mixed NPs. Ablation and irradiation were both carried out in vacuum at a base pressure of 10^{-6} Torr. High-resolution transmission electron microscopy (HRTEM, JEOL 2010F) together with energy dispersive X-ray (EDX) was used to investigate the nanostructure and elemental distribution of the samples. The HRTEM operates at 200 keV with a maximum point-to-point resolution of 0.23 nm, and the spot size of EDX beam is 1 nm in diameter.

3. RESULTS AND DISCUSSION

Figure 1a shows the distribution of a mixture of pure Ag and Ni NPs prepared under optimized ablation conditions. The particles were isolated from each other and the size distribution is shown in Figure 1b. Only particles larger than 10 nm in diameter were counted, and the results show the size of most NPs ranges from 10 to 40 nm.

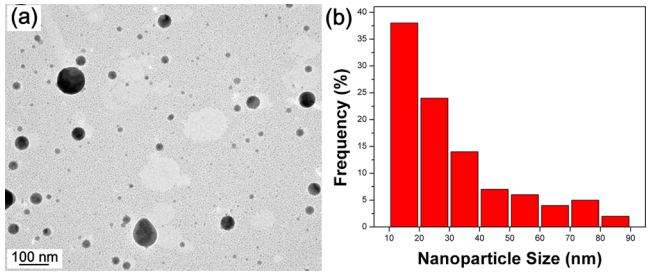

Figure 1. (a) TEM image of a mixture of pure Ag and Ni NPs prior to fs laser irradiation. (b) Size distribution of a mixture of pure Ag and Ni NPs.

HRTEM images of individual NPs display the initial nanostructure of Ag and Ni, as shown in Figure 2a,b. Lattice

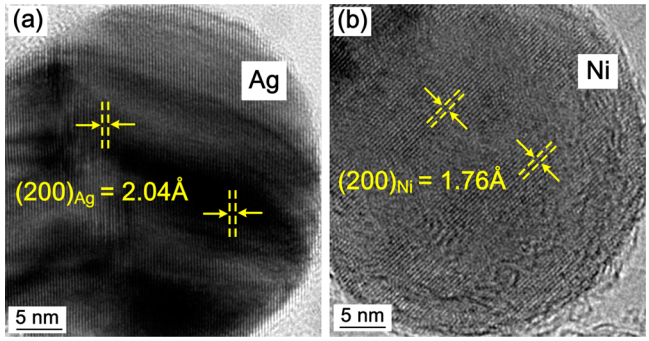

Figure 2. HRTEM images of individual Ag and Ni NPs prior to fs laser irradiation: (a) Ag and (b) Ni.

fringes in these images are marked with white lines. The results indicate that Ag and Ni NPs are each monocrystalline with an interplanar spacing of (200) Ag = 2.04 Å and (200) Ni = 1.76 Å, respectively. No oxidation layer was found in either Ag or Ni NPs.

Figure 3a shows a TEM image of the mixed pure Ag and Ni NPs sample after fs laser irradiation (5 s/5000 overlapping pulses) at a fluence of 1.5 mJ/cm^2. It can be seen that many particles have been joined together compared to the distribution in Figure 1a, which shows only a few cojoined particles.

The composition of joined NPs was analyzed using EDX. Some joined pairs of Ag−Ag and Ni−Ni particles were detected, but joining of dissimilar particles e.g. Ag−Ni pairs was also observed. The inset in Figure 3a shows one joined Ag−Ni NP with EDX line scan positions. Figure 3b shows the high-magnification image of the EDX results. It is clear that no mixing layer is present at the Ag−Ni interface, confirming the formation of a subcluster segregated nanoalloy with only shared bonds at the interface.

As some cojoining of NPs can occur during deposition, a statistical study was carried out to quantitatively determine the effect of fs laser irradiation on the joining of NPs. Ten random squares with the size of 1 μm × 1 μm were analyzed, as shown in Figure 3c. The result of this analysis showed that the number of joined NPs was found to increase by a factor of 4 on average after fs laser irradiation, indicating that laser irradiation enhances the joining of NPs.

Previous studies have discussed fs-laser-induced nanojoining and have demonstrated that the formation of hotspots accompanied by spallation at these locations can result in

dx.doi.org/10.1021/jp506617f | J. Phys. Chem. C 2014, 118, 24746−24751

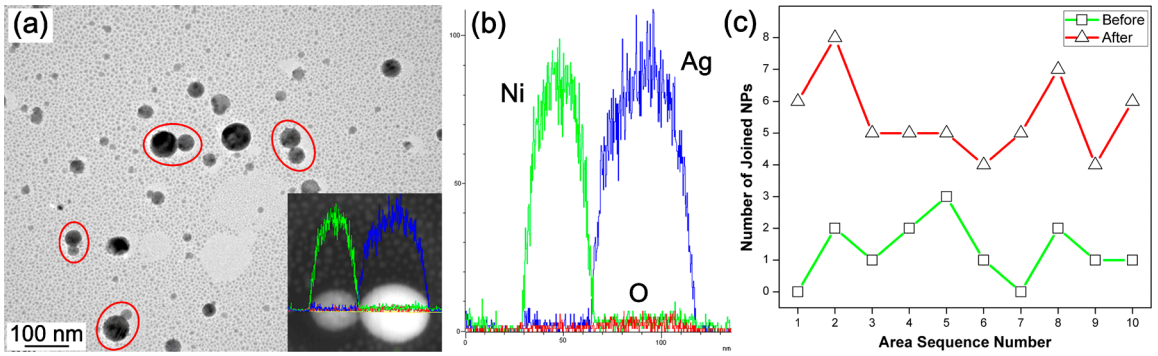

Figure 3. (a) Distribution of a mixture of pure Ag and Ni NPs after fs laser irradiation. The inset shows a high-magnification image of one joined Ag and Ni NP with EDX line scan position. (b) Magnification of EDX data. (c) Statistics of joined NPs in different areas.

atomic intermixing at the interface between NPs of miscible alloys.[13,25] However, for joined Ag−Ni NPs, the EDX results indicate that no intermixing occurs at the Ag−Ni interface. Ossi[26] has investigated surface segregation in transition metal alloys and theoretical predictions indicate that Ag atoms tend to segregate to the surface from Ag−Ni alloys. Nilekar et al.[27] have calculated the segregation energy for impurity atoms and have shown that Ag tends to segregate from Ni due to its negative segregation energy. RapalloIn et al.[7] found that the surface energy of Ag is 78.0 meV $Å^{-2}$, which is nearly half of that of Ni. Consequently, Ag atoms tend to segregate at the surface due to a reduction of surface energy. In addition, a large positive mixing heat was calculated for Ag−Ni,[28] which also indicates that immiscible Ag and Ni atoms tend to segregate from each other. Core−shell segregated Ag−Ni nanoalloys have been confirmed in several experiments.[19,20] The present experiments confirm this behavior and suggest that surface segregation results in the absence of a mixing layer at the interface between joined Ag−Ni NPs. As a result, a Ag−Ni subcluster segregated nanoalloy with shared bonds is formed.

Before characterizing the structure of joined Ag−Ni NPs produced by fs laser irradiation, it is useful to examine the nanostructure of joined NPs with homogeneous composition. The HRTEM images of joined Ag−Ag and Ni−Ni NPs are shown in Figures 4a and 4b, respectively. The white dashed line traces the interface of each joined NPs. The insets show TEM images of the overall morphology. The red squares indicate the area shown in the high-resolution images. The results show that lattice orientation of both particles align in the same direction

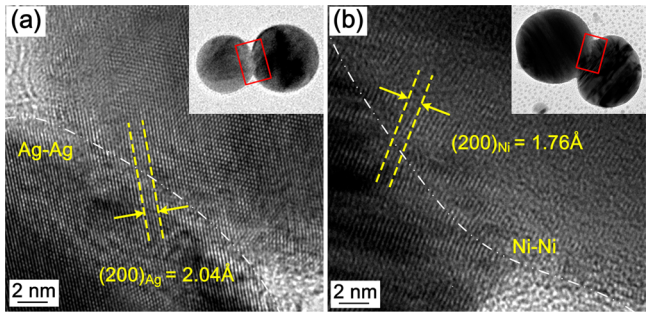

Figure 4. TEM images of joined NPs with homogeneous composition. (a) High-resolution image of the Ag−Ag interface. (b) High-resolution image of the Ni−Ni interface. In each case, the white dashed line traces the interface. Insets show a TEM image of the overall morphology. The red square indicates the area shown in the high-resolution images.

across the interface. This is consistent with our previous studies on the joining Al−Fe NPs, which indicated that the alignment and orientation of lattice planes in joining can be associated with a reduction in surface energy.[13] The results also indicate that there is no oxidation layer in Ag and Ni NPs.

TEM images of the nanostructure in joined Ag and Ni NPs formed by fs laser irradiation are shown in Figure 5a. HRTEM

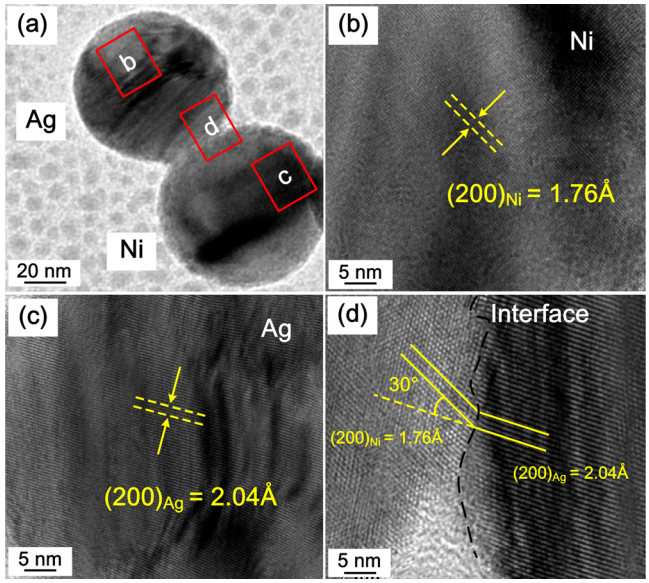

Figure 5. High-resolution TEM images of Ag and Ni NPs joined by exposure to fs laser radiation. (a) Morphology of joined Ag and Ni NPs. The letters show the corresponding high resolution image, and the red squares indicate the corresponding area. (b−d) High-resolution TEM images of the corresponding area.

images of regions within these particles can be seen in Figure 5b−d. The interior of both the Ag and Ni NPs remains monocrystalline with (200) lattice planes. At the interface, the lattice orientations in Ag and Ni were each consistent with that of the interior of the particle. The offset angle between the directions of planes on either side of the interface in joined Ag−Ni particles was found to be ~30°. The interface in joined Ag and Ni NPs did not exhibit a mixed interlayer.

At the interface, the lattice orientations of Ag and Ni were both consistent with that of the interior. The mismatch between (200) Ag and (200) Ni was calculated from

dx.doi.org/10.1021/jp506617f | J. Phys. Chem. C 2014, 118, 24746−24751

$$\delta = \frac{d_1 - d_2}{d_2} \quad (1)$$

where δ is the lattice mismatch and d_1 and d_2 are interplanar spacings in Ag and Ni, respectively. The lattice mismatch between (200) Ag and (200) Ni is then calculated to be 15.91%. Normally, the interface does not have good coherence with such a large lattice mismatch.[29] However, good coherency was found at the Ag−Ni interface, as shown in Figure 3d. Nie et al.[29] found that an irrational oriented interface is parallel to the Moiré plane, which is defined by the intersection between the two sets of planes. In this case, effective continuity of these planes across the interface as well as a one-dimensional coherency within the planar interface can be formed.

The relationship between the two set of Ag−Ni planes is shown schematically in Figure 6. α and β represent the

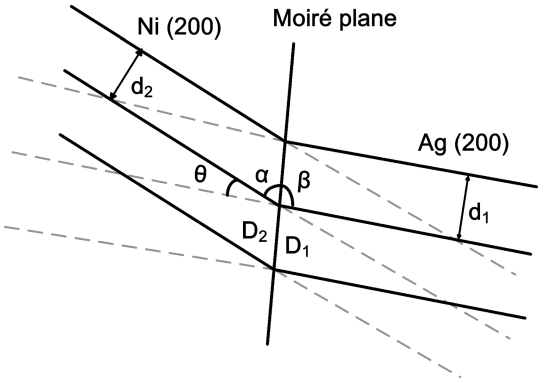

Figure 6. Schematic showing the relationship between the planes of Ni and Ag at the interface.

interplanar angles between the Moiré plane and (200) Ni and (200) Ag, respectively. θ is 30°, which is the observed angle between the two planes, and $\alpha + \beta + \theta = 180°$. α is obtained from eq 2:[30]

$$\alpha = \sin^{-1}\left(\frac{d_1 \sin\theta}{\sqrt{{d_1}^2 + {d_2}^2 - 2d_1d_2\cos\theta}}\right) \quad (2)$$

In the current case, $\alpha = 61°$ and β is calculated to be 89°. If D_1 is the spacing of the (200) plane in Ag parallel to the interface plane, and D_2 is the spacing of the (200) plane in Ni within intersection plane, then

$$D_1 = \frac{d_1}{\sin\alpha} \quad (3)$$

$$D_2 = \frac{d_2}{\sin\beta} \quad (4)$$

Then D_1 = 2.0403 Å, while D_2 = 2.0123 Å. From eq 1, the actual lattice mismatch between (200) Ag and (200) Ni is 1.39%. The small lattice mismatch indicates that the two sets of planes have good coherency at the interface.

The experimental results of Penn et al.[31] show that nanocrystalline TiO_2 particles can also be joined together with oriented attachment. Self-organization of adjacent TiO_2 particles with a number of shared bonds at the interface has been found to reduce the overall surface energy.[32] Simulations of the joining of Ag NPs show that Ag NPs can rotate to lower surface energy.[33] From a thermodynamic point of view, the unique 30° angle at the joined Ag−Ni interface can be associated with a reduction in surface energy.

Figure 7 shows an HRTEM image of the Ag−Ni interface. It can be seen that, although the two sets of planes are well

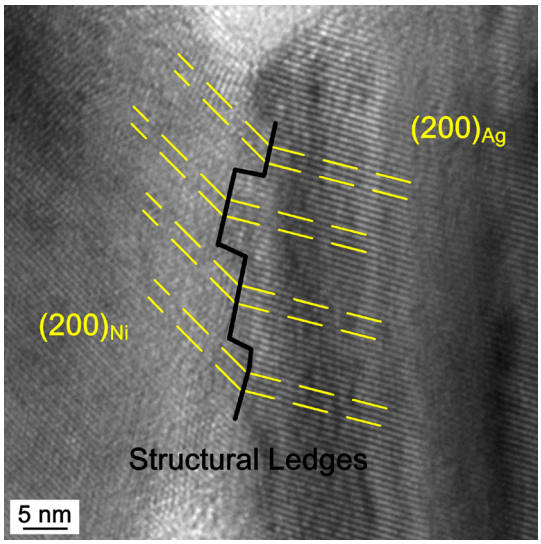

Figure 7. HRTEM image of structural ledges at Ag−Ni interface.

matched, the interface is not a straight line and a set of ledges forms at the interface.

It is well-known that atomic arrangements do not normally match perfectly at the interface of two crystals with different structures. The formation of a structural ledge is one of the misfit accommodation modes at the interphase boundary.[34] Shiflet et al.[35] have found that the presence of structural ledges can compensate atomic misfit at the interface and decrease the defect concentration. As a result, structural ledges are favorable for energy minimization. Mou et al.[36] found structural ledges were formed at irrationally oriented interfaces in Ag−Al alloys to further compensate atomic misfit. Similarly, structural ledges were found at the interface of joined Ag and Ni NPs. It is suggested that these ledges could further compensate for atomic misfit to reduce surface energy. The assumption of a specific angle of 30° as well as the creation of structural ledges minimizes the surface energy facilitating good bonding in Ag and Ni NPs.

For comparison, fs laser joining of Ag−Fe, another immiscible metallic system, has also been investigated. Figure 8a shows TEM scans of joined Ag and Fe NPs after fs laser irradiation. As seen above in the Ag−Ni system, no mixing layer occurs at the interface. In this case, the angle $\theta \approx 35°$ at the Ag−Fe interface (Figure 8b). It is worth noting that there is an oxidation layer on the Fe NP. The oxidation layer only covers part of the Fe N, and is not present across the Ag−Fe interface. This phenomenon indicates that the oxidation layer was formed after the sample was exposed to air, i.e., after joining had occurred.

According to the previous discussion, the calculated angle between the Moiré plane and (200) Ag is 89°, while that with (111) Fe is 56°. The projection distances of (200) Ag and (111) Fe on this plane are calculated to be 2.0403 and 2.0023 Å, respectively, so that the mismatch between (200) Ag and (111) Fe is 1.12%. This small lattice mismatch confirms that the assumption of a specific angle (~35°) is driven by a reduction in surface energy. Furthermore, structural ledges are

dx.doi.org/10.1021/jp506617f | J. Phys. Chem. C 2014, 118, 24746−24751

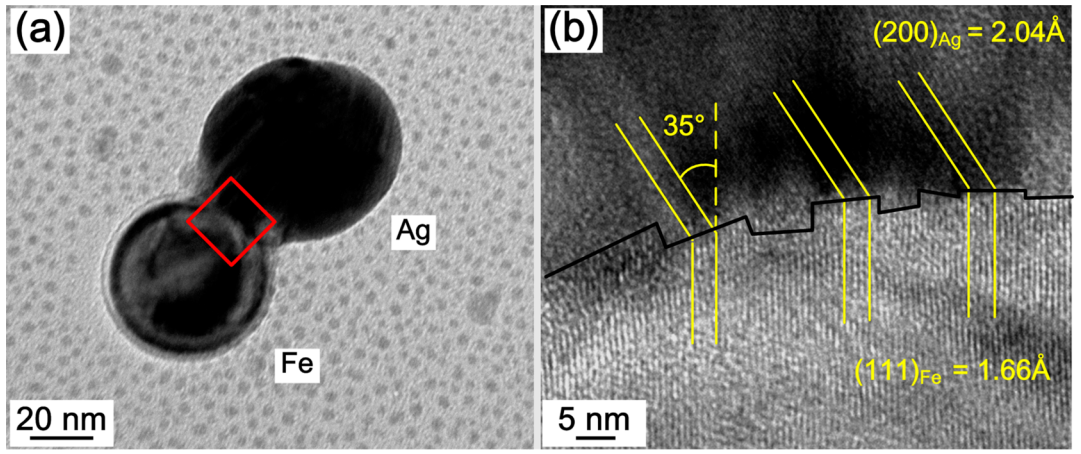

Figure 8. TEM images of Ag and Fe NPs bonded by exposure to fs laser radiation. (a) Morphology of joined Ag and Fe NPs. The red square indicates the high-resolution area. (b) HRTEM image of Ag−Fe interface. The yellow lines display the plane direction, and the black line shows the structural ledges.

also formed at the Ag−Fe interface to further compensate for the mismatch. These results are in good agreement with the mechanisms discussed above.

4. CONCLUSION

The study reported here outlines the first successful experimental approach to the generation of subcluster segregated nanoalloys. This study shows that NPs of immiscible metals can be joined by exposure to fs laser irradiation. Two different systems, consisting of immiscible Ag and Ni, as well as Ag and Fe NPs were successfully joined and nanostructure within and at the interface between individual NPs is discussed. The results show that no mixing layer is found at the interface. Bonding occurs via the formation of a limited number of shared bonds between the two immiscible NPs. The data suggest that surface segregation occurred after fs laser irradiation due to the different surface energy and high mixing heat of the immiscible elements. TEM scans show that a specific angle, driven by the reduction of surface energy, is generated between two matching planes. This interface angle is 30° for (200) Ag//(200) Ni and 35° for (200) Ag//(111) Fe. Calculations show that the angles enable the formation of a low-energy interface with small lattice mismatch. Structural ledges were formed at the Ag−Ni and Ag−Fe interfaces to further compensate atomic misfit.

AUTHOR INFORMATION

Corresponding Authors

*E-mail hepeng@hit.edu.cn (P.H.).
*E-mail nzhou@uwaterloo.ca (Y.N.Z.).

Notes

The authors declare no competing financial interest.

ACKNOWLEDGMENTS

Financial support of National Sciences and Engineering Research Council (NSERC) and State Scholarship Fund of China (No. 201206120144) is gratefully acknowledged. The authors thank Dr. Lei Liu from Department of Mechanical Engineering, Tsinghua University, Dr. Tiesong Lin from State Key Laboratory of Advanced Welding Production Technology, Harbin Institute of Technology, and PhD candidate Hong Huang, Luchan Lin from Centre for Advanced Materials Joining, University of Waterloo, for valuable discussions. The authors thank Dr. Carmen Andrei from the Canadian Centre for Electron Microscopy, McMaster University, for help with TEM operation.

REFERENCES

(1) Shipway, A. N.; Katz, E.; Willner, I. Nanoparticle Arrays on Surfaces for Electronic, Optical, and Sensor Applications. *ChemPhysChem* **2000**, *1*, 18−52.
(2) Sun, S.; Murray, C. B.; Weller, D.; Folks, L.; Moser, A. Monodisperse FePt Nanoparticles and Ferromagnetic FePt Nanocrystal Superlattices. *Science* **2000**, *287*, 1989−1992.
(3) Arrii, S.; Morfin, F.; Renouprez, A. J.; Rousset, J. L. *J. Am. Chem. Soc.* **2004**, *126*, 1199−1205.
(4) Xie, B.; Liu, L.; Peng, X.; Zhang, Y.; Xu, Q.; Zheng, M.; Takiya, T.; Han, M. Optimizing Hydrogen Sensing Behavior by Controlling the Coverage in Pd Nanoparticle Films. *J. Phys. Chem. C* **2011**, *115*, 16161−16166.
(5) Ferrando, R.; Jellinek, J.; Johnston, R. L. Nanoalloys: From Theory to Applications of Alloy Clusters and Nanoparticles. *Chem. Rev.* **2008**, *108*, 845−910.
(6) Ferrer, D.; Torres-Castro, A.; Gao, X.; Sepúlveda-Guzmán, S.; Ortiz-Méndez, U.; José-Yacamán, M. Three-Layer Core/Shell Structure in Au-Pd Bimetallic Nanoparticles. *Nano Lett.* **2007**, *7*, 1701−1705.
(7) Rapallo, A.; Rossi, G.; Ferrando, R.; Fortunelli, A.; Curley, B. C.; Lloyd, L. D.; Tarbuck, G. M.; Johnsto, R. L. Global Optimization of Bimetallic Cluster Structures. I. Size-Mismatched Ag-Cu, Ag-Ni, and Au-Cu Systems. *J. Chem. Phys.* **2005**, *122*, 194308.
(8) Shibata, T.; Bunker, B. A.; Zhang, Z.; Meisel, D.; Vardeman, C. F., II; Gezelter, J. D. Size-Dependent Spontaneous Alloying of Au-Ag Nanoparticles. *J. Am. Chem. Soc.* **2002**, *124*, 11989−11996.
(9) Aguado, A.; López, J. M. Structural and Thermal Behavior of Compact Core-Shell Nanoparticles: Core Instabilities and Dynamic Contributions to Surface Thermal Stability. *Phys. Rev. B* **2005**, *72*, 205420.
(10) Baletto, F.; Mottet, C.; Ferrando, R. Growth Simulations of Silver Shells on Copper and Palladium Nanoclusters. *Phys. Rev. B* **2002**, *66*, 155420.
(11) Kim, H. Y.; Kim, H. G.; Ryu, J. H.; Lee, H. M. Preferential Segregation of Pd Atoms in the Ag-Pd Bimetallic Cluster: Density Functional Theory and Molecular Dynamics Simulation. *Phys. Rev. B* **2007**, *75*, 212105.
(12) Mariscal, M. M.; Dassie, S. A.; Leiva, E. P. M. Collision as a Way of Forming Bimetallic Nanoclusters of Various Structures and Chemical Compositions. *J. Chem. Phys.* **2005**, *123*, 184505.

(13) Jiao, Z.; Huang, H.; Liu, L.; Hu, A.; Duley, W.; He, P.; Zhou, Y. Nanostructure Evolution in Joining of Al and Fe Nanoparticles with Femtosecond Laser Irradiation. *J. Appl. Phys.* **2014**, *115*, 134305.
(14) Jensen, P. Growth of Nanostructures by Cluster Deposition: Experiments and Simple Models. *Rev. Mod. Phys.* **1999**, *71*, 1695−1735.
(15) Hu, A.; Zhou, Y.; Duley, W. W. Femtosecond Laser-Induced Nanowelding: Fundamentals and Applications. *Open Surf. Sci. J.* **2011**, *3*, 42−49.
(16) Chen, J. K.; Qui, J. Q. Patterned 3D Assembly of Au Nanoparticle on Silicon Substrate by Colloid Lithography. *J. Nanopart. Res.* **2012**, *14*, 942.
(17) Zhou, Y.; Hu, A. From Microjoining to Nanojoining. *Open Surf. Sci. J.* **2011**, *3*, 32−41.
(18) Ma, E. Alloys Created Between Immiscible Clements. *Prog. Mater. Sci.* **2005**, *50*, 413−509.
(19) Portales, H.; Saviot, L.; Duval, E.; Gaudry, M.; Cottancin, E.; Pellarin, M.; Lermé, J.; Broyer, M. Resonant Raman Scattering by Quadrupolar Vibrations of Ni-Ag Core-Shell Nanoparticles. *Phys. Rev. B* **2002**, *65*, 165422.
(20) Gaudry, M.; Cottancin, E.; Pellarin, M.; Lermé, J.; Arnaud, L.; Huntzinger, J. R.; Vialle, J. L.; Broyer, M. Size and Composition Dependence in the Optical Properties of Mixed (Transition Metal/Noble Metal) Embedded Clusters. *Phys. Rev. B* **2003**, *67*, 155409.
(21) Wang, P.; Huang, B.; Daia, Y.; Whangbob, M. Plasmonic Photocatalysts: Harvesting Visible Light with Noble Metal Nanoparticles. *Phys. Chem. Chem. Phys.* **2012**, *14*, 9813−9825.
(22) Langlois, C.; Li, Z. L.; Yuan, J.; Alloyeau, D.; Nelayah, J.; Bochicchio, D.; Ferrando, R.; Ricolleau, C. Transition from Core−Shell to Janus Chemical Configuration for Bimetallic Nanoparticles. *Nanoscale* **2012**, *4*, 3381−3388.
(23) Gonzalez, J. J.; Liu, C.; Wen, S. B.; Mao, X.; Russo, R. E. Metal Particles Produced by Laser Ablation for ICP-MS Measurements. *Talanta* **2007**, *73*, 567−576.
(24) Alves, S.; Kalberer, M.; Zenobi, R. Direct Detection of Particles Formed by Laser Ablation of Matrices during Matrix-Assisted Laser Desorption/Ionization. *Rapid Commun. Mass Spectrom.* **2003**, *17*, 2034−2038.
(25) García-Navarro, A.; Agulló-López, F.; Olivares, J.; Lamela, J.; Jaque, F. Femtosecond Laser and Swift-Ion Damage in Lithium Niobate: A Comparative Analysis. *J. Appl. Phys.* **2008**, *103*, 093540.
(26) Ossi, P. M. Surface Segregation in Transition-Metal Alloys - Experiments and Theories. *Surf. Sci.* **1988**, *201*, L519−L531.
(27) Nilekar, A. U.; Ruban, A. V.; Mavrikakis, M. Surface Segregation Energies in Low-Index Open Surfaces of Bimetallic Transition Metal Alloys. *Surf. Sci.* **2009**, *603*, 91−96.
(28) Li, Z. C.; Yu, D. P.; Liu, B. X. Manipulation of Ordered Layered Structures by Interface-Assisted Ion-Beam Mixing in Immiscible Ag-Co and Ag-Ni Systems. *Phys. Rev. B* **2002**, *65*, 245403.
(29) Fredriksson, H.; Akerlind, U. *Solidification and Crystallization Processing in Metals and Alloys*; Royal Institute of Technology: Stockholm, Sweden, 2012.
(30) Nie, J. F.; Muddle, B. C. Orientation and Structure of Planar Facets on the Massive Phase γ_m in a Near-TiAl Alloy. *Metall. Mater. Trans. A* **2002**, *33*, 2381−2389.
(31) Penn, R. L.; Banfield, J. F. Imperfect Oriented Attachment: Dislocation Generation in Defect-Free Nanocrystals. *Science* **1998**, *281*, 969−971.
(32) Penn, R. L.; Banfield, J. F. Morphology Development and Crystal Growth in Nanocrystalline Aggregates under Hydrothermal Conditions: Insights from Titania. *Geochim. Cosmochim. Acta* **1999**, *63*, 1549−1557.
(33) Marzbanrad, E.; Hu, A.; Zhao, B.; Zhou, Y. Room Temperature Nanojoining of Triangular and Hexagonal Silver Nanodisks. *J. Phys. Chem. C* **2013**, *117*, 16665−16676.
(34) Vandermerwe, J. H.; Shiflet, G. J.; Stoop, P. M. Structural Ledges in Interphase Boundaries. *Metall. Mater. Trans. A* **1991**, *22*, 1165−1175.
(35) Shiflet, G. J.; Vandermerwe, J. H. The Role of Structural Ledges as Misfit-Compensating Defects: fcc-bcc Interphase Boundaries. *Metall. Mater. Trans. A* **1994**, *25*, 1895−1903.
(36) Mou, Y. W.; Aaronson, H. I. Interphase Boundary Structures Associated with the β to ξ_m Massive Transformation in a Ag-26 at.% Al-Alloy. *Acta Metall. Mater.* **1994**, *42*, 2159−2173.